ACS APPLIED MATERIALS & INTERFACES

Research Article

www.acsami.org

Enzymatic Functionalization of Cork Surface with Antimicrobial Hybrid Biopolymer/Silver Nanoparticles

Antonio Francesko,[†,#] Lucas Blandón,[‡,#] Mario Vázquez,[‡] Petya Petkova,[†] Jordi Morató,[§] Annett Pfeifer,[∥] Thomas Heinze,[∥] Ernest Mendoza,[⊥] and Tzanko Tzanov*[,†]

[†]Grup de Biotecnologia Molecular i Industrial, Department of Chemical Engineering, Universitat Politècnica de Catalunya, 08222 Terrassa, Spain

[‡]Grupo Interdisciplinario de Estudios Moleculares, Instituto de Química, Universidad de Antioquia, Medellín, Colombia

[§]AQUASOST Group - UNESCO Chair on Sustainability, Universitat Politècnica de Catalunya, 08034 Barcelona, Spain

[∥]Center of Excellence for Polysaccharide Research, Institute of Organic Chemistry and Macromolecular Chemistry, Friedrich Schiller University of Jena, 07743 Jena, Germany

[⊥]Grup de Nanomaterials Aplicats. Centre de Recerca en Nanoenginyeria, Universitat Politècnica de Catalunya, 08222 Terrassa, Spain

ABSTRACT: Laccase-assisted assembling of hybrid biopolymer−silver nanoparticles and cork matrices into an antimicrobial material with potential for water remediation is herein described. Amino-functional biopolymers were first used as doping agents to stabilize concentrated colloidal dispersions of silver nanoparticles (AgNP), additionally providing the particles with functionalities for covalent immobilization onto cork to impart a durable antibacterial effect. The solvent-free AgNP synthesis by chemical reduction was carried out in the presence of chitosan (CS) or 6-deoxy-6-(ω-aminoethyl) aminocellulose (AC), leading to simultaneous AgNP biofunctionalization. This approach resulted in concentrated hybrid NP dispersion stable to aggregation and with hydrodynamic radius of particles of about 250 nm. Moreover, laccase enabled coupling between the phenolic groups in cork and amino moieties in the biopolymer-doped AgNP for permanent modification of the material. The antibacterial efficiency of the functionalized cork matrices, aimed as adsorbents for wastewater treatment, was evaluated against *Escherichia coli* and *Staphylococcus aureus* during 5 days in conditions mimicking those in constructed wetlands. Both intrinsically antimicrobial CS and AC contributed to the bactericidal effect of the enzymatically grafted on cork AgNP. In contrast, unmodified AgNP were easily washed off from the material, confirming that the biopolymers potentiated a durable antibacterial functionalization of the cork matrices.

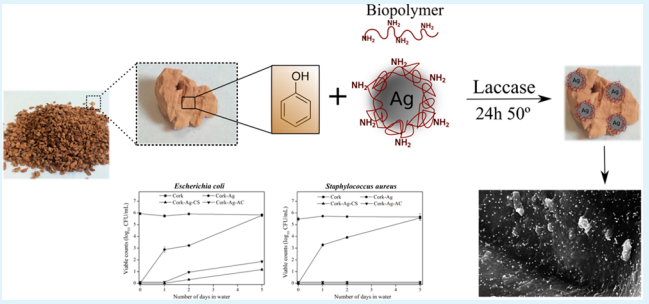

KEYWORDS: *amino-functional biopolymers, silver nanoparticles, cork, enzymatic grafting, antimicrobial activity*

1. INTRODUCTION

Inadequate waste treatment and poor infrastructure for water disinfection are threats to water quality and public health through disease outbreaks globally. Many decontamination strategies have been implemented with different success for reducing the impact of water pollution. Constructed wetlands in various designs are the most versatile systems for removal of pesticides, heavy metals, polycyclic aromatic compounds, and pharmaceutical residues.[1−4] Currently, a major issue with these systems is related to the additional microbial contamination, especially the growth of undesired pathogen bacteria. Reutilization of the water treated in wetlands, e.g., for irrigation, requires its previous microbial decontamination to meet the agricultural quality standards. In Spain, for example, a maximum of 100 UFC of *Escherichia coli* per 100 mL of irrigation water is recommended. Nowadays, the development of efficient materials for microbiological remediation of wastewaters is being intensively investigated.[5,6] Silver nanoparticles (AgNP) are largely claimed as broad-spectrum antibacterial agents, whose efficacy depends on their size and morphology. While the mechanism of their antibacterial activity remains a subject of debate, the most widely accepted one involves the perturbation of the bacterial cell wall by the NP, resulting in cell death.[7,8]

Chemical reduction, electrochemistry, sonochemistry, and laser ablation are versatile methods for the synthesis of AgNP. If produced in low concentration, AgNP colloidal dispersions are stable for months. However, the concentrated dispersions, usually applied to achieve the desired antibacterial effect, require stabilizers due to NP coalescence.[9] In this light, stabilizing agents for particle surface passivation are explored to reduce the AgNP aggregation. Although these agents vary from

Received: February 22, 2015
Accepted: April 20, 2015
Published: April 20, 2015

DOI: 10.1021/acsami.5b01670
ACS Appl. Mater. Interfaces 2015, 7, 9792−9799

simple molecules to polymers, their common feature is the hydrophobic interaction with the NP surface.[10,11] Some frequently reported AgNP stabilizers are cetylammonium bromide, tetrabutylammonium acetate, poly(vinylpirrolidone), and biopolymers, such as chitosan.[12]

Due to their structural diversity and chemical functionality, biopolymers are considered advantageous for stabilization of metal NP, in addition to being biocompatible and biodegradable. For example, those bearing amino moieties are intrinsically antimicrobial and impart positive charge onto the metal surface to lower the particle aggregation over a wide pH range, thereby extending the shelf life of these systems.[13,14] Moreover, the inclusion of amino functionalities brings about reactivity to the otherwise inert metal NP, necessary for permanent immobilization of the hybrid biopolymer−metal NP onto different surfaces. Covalent immobilization on solid substrates is employed to facilitate not only the recovery but also the NP reuse.[13,15]

One potentially attractive and largely available material for AgNP immobilization is the residual cork, mainly from the cork stoppers industry in Mediterranean countries. Granulated or powdered cork particles have remarkable sorption capacity due to their porous surface and chemical composition[16,17] and thus can be used for adsorptive removal of organic pollutants and heavy metals in waste waters. The chemical composition of cork depends on its origin and varies between 40 and 60% suberin, 10−50% lignin, 5−15% polysaccharides, and 10−25% extractable components including waxes and tannins.[18,19] Lignin, suberin, and tannin molecules possess a large number of phenolic moieties, which can be enzymatically oxidized into reactive quinones that can further react with nucleophiles such as the amino groups of the biopolymers via 1,4-Michael addition or Schiff base formation. The enzymatic coupling on cork of the hybrid biopolymer−NP antibacterial systems offers advantages over chemical conjugation in terms of high specificity and mild reaction conditions. Phenoloxidases, such as tyrosinases and laccases, are enzymes capable of promoting the grafting process.[20] These enzymatic tools have been shared by other applications developed in our group, including lignin-based adhesives for floor coverings,[21] antimicrobial and shrink-resistant wool,[22] permanent dyeing of cotton,[23] antifouling coatings on urinary catheters,[24] and biopolymer hydrogels for wound dressing,[25] thus demonstrating the versatility of the enzymatic grafting approach.

In this study AgNP colloidal dispersions were synthesized by reduction of $AgNO_3$ with $NaBH_4$ and simultaneously doped with two amino-functional biopolymers: chitosan and 6-deoxy-6-(ω-aminoethyl) aminocellulose. In this reaction the chemical reagent can be omitted because both CS and AC have been used as combined reducing and capping agents.[26,27] We used $NaBH_4$ as a fast reducing agent in order to avoid high temperatures in the reaction and/or the assistance of an additional technology required for the Ag^+ reduction. Our goal was to permanently graft the hybrid Ag−biopolymer systems on the surface of cork in which case the nonattached particles and the excess of $NaBH_4$ are easily removed by thorough washing. Therefore, laccase-assisted oxidation of the phenolic structures in cork was used to covalently immobilize the hybrid biopolymer−AgNP on the cork surface via reaction with the amino groups in biopolymers. The antimicrobial activity of the green-functionalized cork was evaluated against *Escherichia coli* and *Staphylococcus aureus*, in order to assess its potential as a filter to reduce these common pathogenic indicators of pollution in constructed wetlands.

2. EXPERIMENTAL SECTION

2.1. Materials, Reagents, and Bacteria. Granulated cork with mean particle size of ∼0.5 cm was provided by the Catalan Cork Institute. Silver nitrate ($AgNO_3$), sodium borohydride ($NaBH_4$), hydrochloric acid, sodium hydroxide, and ethanol were of analytical grade, purchased from Sigma-Aldrich (Spain). Laccase (EC 1.10.3.2 *Trametes* sp. laccase, Laccase L603P) was provided by Biocatalysts, UK. Laccase activity was determined by oxidation of 5 mM 2,2′-azino-bis(3-ethylbenzthiazoline-6-sulfonic acid) (ABTS) substrate in 0.1 M succinic acid/succinate buffer (pH 5.0), followed by an absorbance increase at 420 nm and 50 °C, to obtain 0.14 U mg^{-1} protein, where one unit is defined as the amount of enzyme necessary to oxidize 1 μmol of ABTS per min (ε_{420} = 36 000 M^{-1} cm^{-1}). Protein content was determined using the Bradford method, obtaining 0.125 mg of protein per mg of solid. The two amino-containing biopolymers used in the study were medical grade chitosan (CS, ∼15 kDa, DDA 87%) obtained from Kitozyme (Belgium) and 6-deoxy-6-(ω-aminoethyl) aminocellulose (AC, ∼15 kDa). Microcrystalline cellulose (Fluka, Avicel PH-101) dried at 105 °C for 2 h was used for the AC preparation. First, tosyl cellulose was prepared using the synthesis method of Rahn et al.,[28] obtaining the product with a degree of substitution (DS) of 0.8. Ethylenediamine was then added in excess, and the mixture was stirred for 3 h at 100 °C. After precipitation in H_2O the conjugate was filtered, washed several times with isopropanol and H_2O, and finally dried in vacuum. Gram-positive *Staphylococcus aureus* (*S. aureus*, ATCC 25923) and Gram-negative *Escherichia coli* (*E. coli*, ATCC 25922) were used for the antimicrobial assays. Plate count agar and other reagents for cell culture studies were purchased from Sigma-Aldrich unless otherwise specified.

2.2. Methods. *Preparation of Biopolymer-Doped Ag Nanoparticles.* Biopolymers were dissolved to reach 0.8% (w/v) in 1% CH_3COOH (CS) and distilled water (AC). The pH of the solutions was adjusted to 5 by adding 2 M NaOH in the case of CS and 1 M HCl in the case of AC. AgNP synthesis was carried out by chemical reduction of Ag^+ to elemental Ag using $NaBH_4$ (17.5 mg/mL in dH_2O), starting from aqueous solutions of $AgNO_3$ (5 mg/mL) in the presence of CS or AC. First, 2 mL of $NaBH_4$ was added to 30 mL of a biopolymer solution under vigorous stirring, and then $AgNO_3$ was slowly added to reach the final volume of 50 mL.

Characterization of Biopolymer-Doped Ag Nanoparticles. The hybrid structures were characterized using ζ potential for the particle charge, dynamic light scattering (DLS) for the mean particle size, UV−vis spectrophotometry to check for the presence and intensity of the AgNP surface plasmon resonance (SPR) band, and scanning transmission electron microscopy (STEM) to visualize the particles and evaluate their stability in the obtained dispersions. ζ potential was measured using a Malvern Zetasizer Nano ZS, and DLS measurements were performed using a DL135 Particle Size Analyzer (Cordouan Technologies, France). Three samples of each AgNP dispersion (in the absence and presence of CS of AC) were processed acquiring five measurement cycles with 1% signal-to-noise ratio. The data were analyzed using NanoQ 1.2.1.1 software. UV−visible spectra were recorded between 300 and 600 nm for the dispersions diluted 100 times in distilled water using a Cary 100 Bio spectrophotometer (Varian). The AgNP in the dispersions were visualized by a Zeiss Neon FIB microscope (Carl Zeiss, Germany) in STEM mode operating at 30 kV acceleration voltage. The samples for observation were drop-casted on a TEM holey carbon grid.

Immobilization of the Hybrid Biopolymer-Doped AgNP onto Cork. Prior to the treatment with biopolymer-doped AgNP, the cork granules were cleaned with aqueous solution of HCl (pH 2), distilled H_2O, NaOH solution (pH 10), and finally 96% EtOH and dried at 60 °C for 12 h. Thereafter, 1 g of the material was placed in a mixture containing 18 mL of AgNP dispersion (pure, doped with CS, or doped with AC − immediately after their preparation), 18 mL of 0.1 M succinic acid/succinate buffer (pH 5), and 0.5 mL of laccase (final

DOI: 10.1021/acsami.5b01670
ACS Appl. Mater. Interfaces 2015, 7, 9792−9799

concentration 0.1 U/mL). The reaction was allowed to proceed for 24 h at 50 °C and 30 rpm in a laboratory dying machine Ahiba (Datacolor). Control samples were also prepared using the same treatment conditions without laccase (in the presence of hybrid biopolymer−AgNP) and with laccase and CS or AC alone (without AgNP). The treated cork was washed thoroughly with water to remove the loosely fixed particles and $NaBH_4$ from the material and finally dried at 50 °C for 12 h.

Fourier transform infrared spectroscopy (FTIR) was used to analyze the surface of the treated cork. IR spectra of the samples were collected in the range of 4000−600 cm^{-1} using a PerkinElmer Spectrum 100 (USA) equipped with universal ATR sampling accessory, performing 64 scans for each spectrum. Scanning electron microscopy (SEM) was performed to examine the morphology of the AgNP−biopolymer hybrids immobilized onto cork. The micrographs with magnification ×30K were obtained using a Zeiss Neon FIB microscope (Carl Zeiss, Germany) operating in SEM mode.

Antimicrobial Activity of AgNP Embedded Cork Matrices. The antimicrobial performance of treated cork matrices was assessed against *E. coli* and *S. aureus* using the dynamic shake ASTM E 2149-01 test, as described by Petkova et al.[29] The results were expressed as $\log_{10}$ of colony forming units (CFU) per milliliter of buffer solution in the flask. Besides the unwashed matrices (only rinsed with water after the treatment), the antibacterial performance of the untreated and treated cork was evaluated after immersing those in water for 1, 2, and 5 days at room temperature while stirring (100 rpm) to mimic the environment in which the materials are intended to be used, i.e., water flow in constructed wetlands. Finally, the antimicrobial activity after 5 days washing is also expressed as a reduction percentage of the survived bacteria colonies, calculated as follows

$$\text{Reduction}\ (\%) = (A - B)/A \times 100$$

where A represents the number of colonies (CFU) survived from the dispersion that was not in contact with cork and B represents CFU for the dispersions in contact with the untreated and functionalized cork material. These values were also compared with the cork enzymatically treated with only biopolymers (solutions not containing AgNP).

3. RESULTS AND DISCUSSION

3.1. Characterization of AgNP and AgNP−Biopolymers Dispersions. AgNP were synthesized by a chemical reduction of $AgNO_3$ with $NaBH_4$ in the absence and presence of biopolymers. In order to confirm the interactions between CS and AC with AgNP during their synthesis, the ζ potential of pure AgNP and biopolymer-doped AgNP was measured. AgNP doped with biopolymers displayed positive ζ potential values due to the presence of amino groups in the macromolecules that are protonated at pH 5—used for the AgNP preparation (Table 1). Given that pure AgNP display a negative potential, these results suggest the interactions between the AgNP and the biopolymers.

The pure AgNP also displayed notably smaller hydrodynamic radius than their homologues doped with biopolymers (Table 1). When measured by DLS, the increase in the NP diameter in the presence of biopolymers represents an indirect demonstration that the AgNP are coated with macromolecules in thick layers.[13] This is the opposite of a thin-layer doping of noble metal nanoparticles in which case the change in the hydrodynamic radius is negligible.[10] Also, in our study it is probable that the similar Mw of the biopolymers used induced comparable size increase after the AgNP doping.

Table 1. ζ Potential and Mean Hydrodynamic Radius of AgNP Synthesized in the Absence and Presence of CS and AC

sample	ζ potential (mV)	mean particle size (nm)
AgNP	−25.3 ± 0.8	32.3 ± 1.7
AgNP-CS	41.5 ± 0.7	239.6 ± 13.5
AgNP-AC	26.2 ± 1.36	253.8 ± 20.0

The interactions between the AgNP and biopolymers were further confirmed by STEM analysis. Without doping the AgNP were abundant in the dispersion, and most of the particles displayed the sizes ≤30 nm (Figure 1A). In contrast, the average sizes of the AgNP doped with CS or AC, which were shaped in rod-like structures, exceeded 100 nm, thereby confirming the DLS findings (Figure 1B and 1C). The doped particles were well dispersed in the biopolymer templates forming aggregated complexes, apparently as a result of their sticking upon drying of the sample. The pure AgNP precipitated in a matter of hours leaving very few particles in the dispersion (Figure 1D). This is expected since the synthesis of nanoparticles by strong chemical reduction often results in agglomeration and precipitation of the colloids. In contrast, the hybrid structures of the biopolymer-doped AgNP were stable and resisted the aggregation in dispersion and precipitation (Figure 1E and 1F). STEM images together with the macroscopic observation of the dispersions (inset images) provided a clear proof that both CS and AC stabilized the AgNP dispersions through the passivation of the particle surface.

UV−vis spectra were recorded for the pure AgNP and the dispersions doped with CS and AC after 72 h of their synthesis. Since the dispersion prepared in the absence of biopolymers was unstable and entirely precipitated during this time leaving the above solution clear, no characteristic for AgNP absorption is observed in its spectrum in the 300−500 nm range (Figure 2). In contrast, the SPR band was detected for the stable AgNP dispersions prepared in the presence of both CS and AC. The change in color of the dispersion and the consequent appearance of the bands between 400 nm (for AgNP−AC) and 425 (for AgNP−CS) implies the interaction between the biopolymers and AgNP surface which modify their interaction with light.[30]

Besides the different wavelength position of the SPR peak, the intensity of AgNP−AC was around 3 times higher than that of AgNP−CS. The intensity of the band in the AgNP systems where biopolymers are used as particle stabilizers varies as a function of the preparation conditions, as well as the amount of a biopolymer used for the particle doping. Nevertheless, despite the higher peak intensity of the AgNP−AC system and the same starting concentrations of AC and CS, it still could not be concluded that this macromolecule interacts better with silver compared to CS, especially in the case where the reduction of Ag^+ to elemental silver solely depends on the chemical compound ($NaBH_4$). Although the peak intensities are directly proportional to the amount of the AgNP−biopolymer hybrids, these can only be compared between different samples of the same system (obtained varying the preparation conditions). For example, certain biopolymer concentrations can decrease the Ag particle surface exposure to light, which may be the reason for the decrease or even the absence of the SPR band in such systems.[31] If such a scenario is applied to our case, we may even speculate on a better coverage of the AgNP surface by CS compared to AC due to their strong interactions. Nevertheless, the strength of the organic−inorganic interactions as a function of the biomaterial structure goes beyond the scope of this manuscript.

DOI: 10.1021/acsami.5b01670
ACS Appl. Mater. Interfaces 2015, 7, 9792−9799

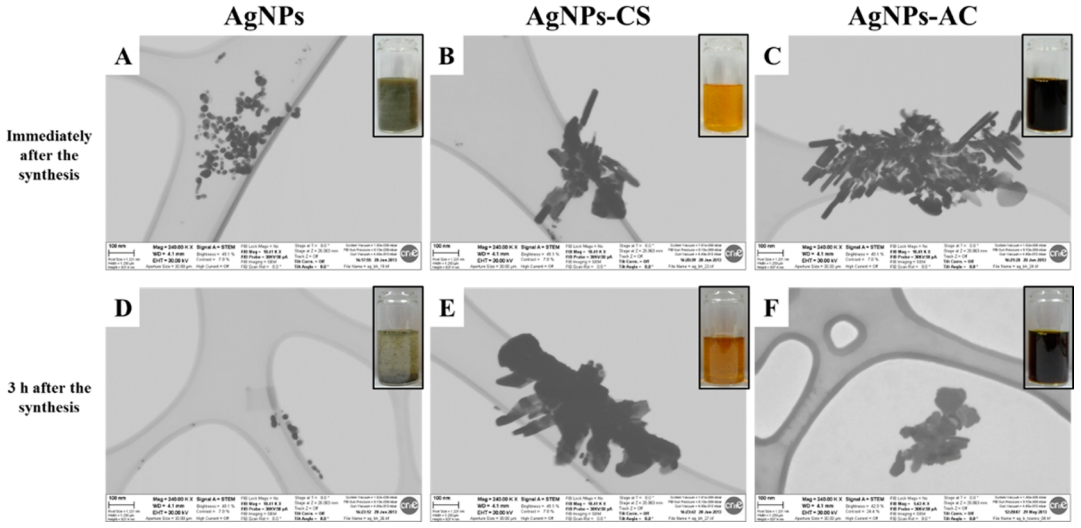

Figure 1. STEM images of the AgNP dispersions synthesized in the absence and presence of CS and AC. The images were taken to evaluate the presence of nanoparticles in the dispersions immediately after the synthesis of the particles (images A, B, and C) and after 3 h of their preparation (images D, E, and F). The inset photographs represent the analyzed dispersions.

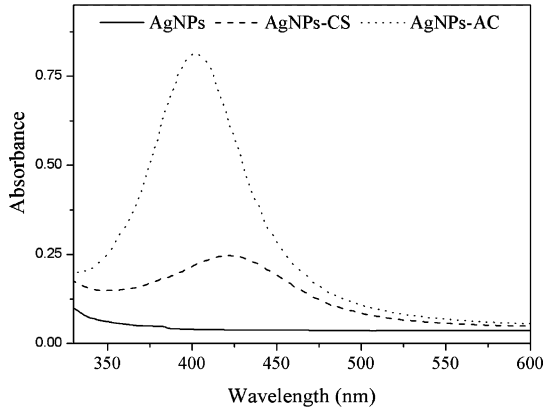

Figure 2. UV−vis spectra obtained for the pure AgNP dispersion and the dispersions doped with CS and AC after 72 h of their synthesis.

Important from the technological point of view, the uniform color distribution throughout both AgNP−CS and AgNP−AC dispersions means that these hybrid systems were uniformly distributed in the dispersions, which broadens their application potential and facilitates exploitation of their functional properties. In addition, no precipitation was observed during several weeks after their synthesis, revealing sufficient stability of the systems for, e.g., further surface functionalization of different materials.

3.2. Enzymatic Grafting of Hybrid Biopolymer−AgNP on Cork. The characterization of the AgNP and hybrid biopolymer−AgNP using ζ potential, DLS, UV−vis, and STEM analysis indicated that interactions between the particles and CS or AC occur. Doping of the AgNP with these biopolymers provides the amino moieties on the particle surface necessary for the enzyme-catalyzed covalent immobilization of NP onto cork. The used enzymatic immobilization approach is complex

Scheme 1. Mechanism of Immobilization of the Hybrid AgNP−Biopolymers onto Cork[a]

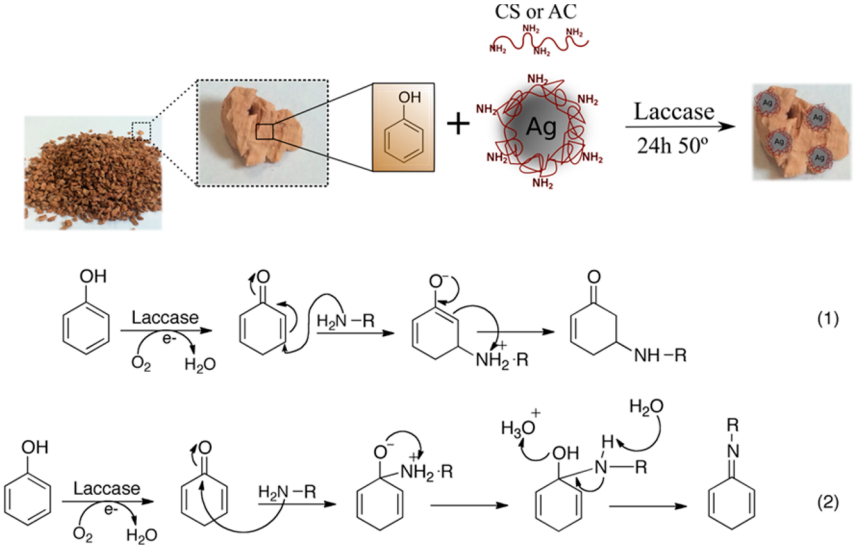

[a]Mechanisms above the scheme show two possibilities of reaction: (1) Michael addition, (2) Schiff base formation.

DOI: 10.1021/acsami.5b01670
ACS Appl. Mater. Interfaces 2015, 7, 9792−9799

and may involve different interactions/reactions between the cork surface and used macromolecules, such as electrostatic interactions, hydrogen bonding, and covalent linking between the laccase-activated cork moieties and CS or AC. In this work we targeted covalent bonding in order to permanently functionalize the cork surface with biopolymer-doped AgNP using laccase-assisted immobilization which necessarily comprises: (i) oxidation of the cork phenol groups (from suberin and lignin) to reactive quinones and (ii) reaction of the quinones with nucleophilic moieties (amino groups) in biopolymers through 1,4-Michael addition or Schiff base formation,[25] as illustrated in Scheme 1.

FTIR spectra were recorded to verify whether the functionalization of the cork surface was successful. Prior to analysis, unmodified cork, cork enzymatically treated with pure AgNP (immediately after their preparation), and cork treated with the hybrid biopolymer−AgNP were subjected to thorough washing during which the samples were immersed in distilled water and vigorously stirred for 5 days. The water was changed each 24 h, and the remaining solutions were checked for the presence of nanoparticles by optical microscopy using a Nikon Eclipse Ti microscope, with a 100× oil-immersion objective. After 4 days in water, no particles were detected in any of the remaining solutions meaning that after this time there was no AgNP leaching from the samples.

The unmodified cork and cork treated with pure AgNP displayed characteristic for cork spectra with some of the most prominent bands as markers of: (i) suberin at 1462, 1236, and 1157 cm^{-1}, its aliphatic chains at 2918 and 2852 cm^{-1}, and its ester groups at 1735 and 721 cm^{-1}, (ii) lignin aromatics at 1600, 1510, and 849 cm^{-1}, and (iii) cork polysaccharides at 1096 and 1035 cm^{-1} (Figure 3).[32] Clear and comparable

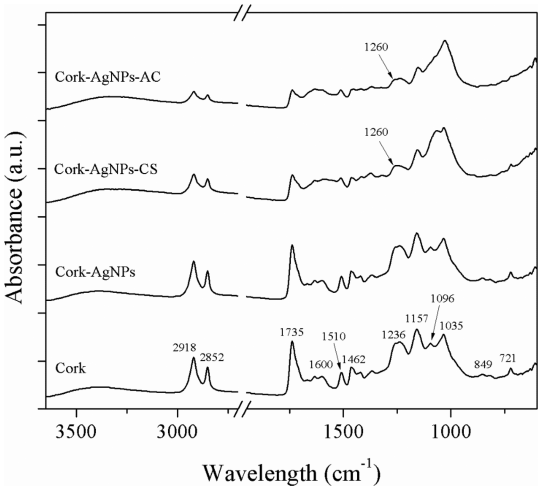

Figure 3. FTIR−ATR spectra of untreated and enzymatically functionalized cork with AgNP, AgNP−CS, and AgNP−AC dispersions.

differences were found in the spectra of the cork treated with AgNP−biopolymer hybrids. All peaks attributed to the cork suberin including the bands constituting the typical suberin fingerprint (1462, 1236, and 1157 cm^{-1})[33] decreased considerably after the enzymatic functionalization. Also the bands representing the lignin aromatics decreased or completely disappeared. Thus, both suberin and lignin from cork were involved in the functionalization reaction. At the same time, the differences in the spectra in polysaccharide regions between 1532−1681 cm^{-1} and 900−1120 cm^{-1} suggest a successful biopolymer grafting, but these regions are rather complicated for deeper analysis. Instead, a shoulder peak was noticed at 1260 cm^{-1} in the spectra of the treated cork (especially pronounced for the cork treated with AgNP−CS), which could be attributed to C−N stretching of aryl amides formed via Michael addition.[25] Therefore, the FTIR spectra confirmed that the phenolic moieties from suberin and lignin in cork were covalently linked with CS or AC, where the reaction occurred predominantly via Michael addition.

SEM analysis was carried out in order to confirm the presence of AgNP on the cork surface after the enzymatic treatment. On average, cork cells rarely exceed 50 μm height, with a hexagonal face of 15−20 μm and a thickness of 1−2 μm.[17] SEM images were thus taken inside the cells, first for the untreated cork without the NP (Figure 4A). The cell surface

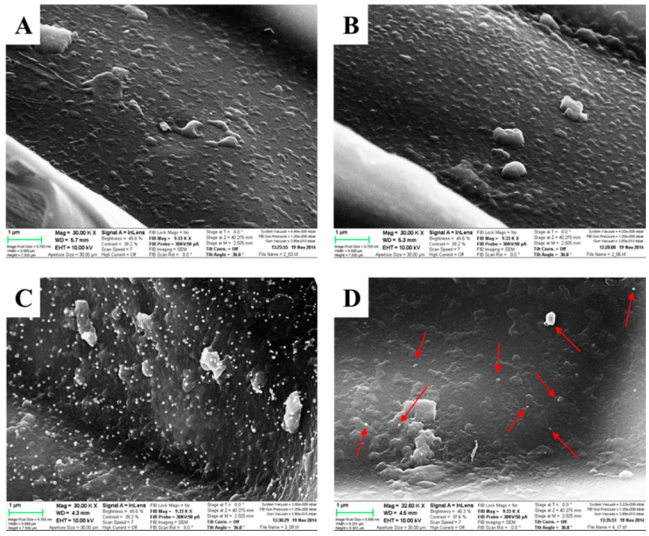

Figure 4. SEM images of cork surface enzymatically treated in the absence (A) and presence of nanoparticles: (B) pure AgNP, (C) AgNP−AC, and (D) AgNP−CS.

was not smooth and appeared granulated, where the remaining deposits, not removed during the cleaning procedure, were noticed. The same deposits were observed on the cork treated in the presence of laccase with the AgNP immediately after their synthesis (Figure 4B). The AgNP were thus not fixed on the cork surface or were removed during the immersion in water for 5 days. In contrast, particles and macromolecular structures were observed on the cork enzymatically embedded with the hybrid AgNP−biopolymer systems even after extensive washing with water (Figure 4C and 4D). This was especially the case of AgNP−CS treated cork, which displayed a large amount of NP on the surface. Both individual submicron particles and larger agglomerates could be visualized. A lower number of AgNP was observed on the cork surface treated with the AgNP−AC system (marked with red arrows on Figure 4D), but these were still fixed strong enough to resist the removal by thorough washing. A larger number of permanently deposited AgNP was achieved via the laccase-assisted grafting of CS on cork.

3.3. Antimicrobial Activity of AgNP-Embedded Cork Matrices. The antibacterial activity of cork matrices functionalized with biopolymer-doped AgNP was evaluated at different time points after immersing the materials in water up to 5 days.

DOI: 10.1021/acsami.5b01670
ACS Appl. Mater. Interfaces 2015, 7, 9792−9799

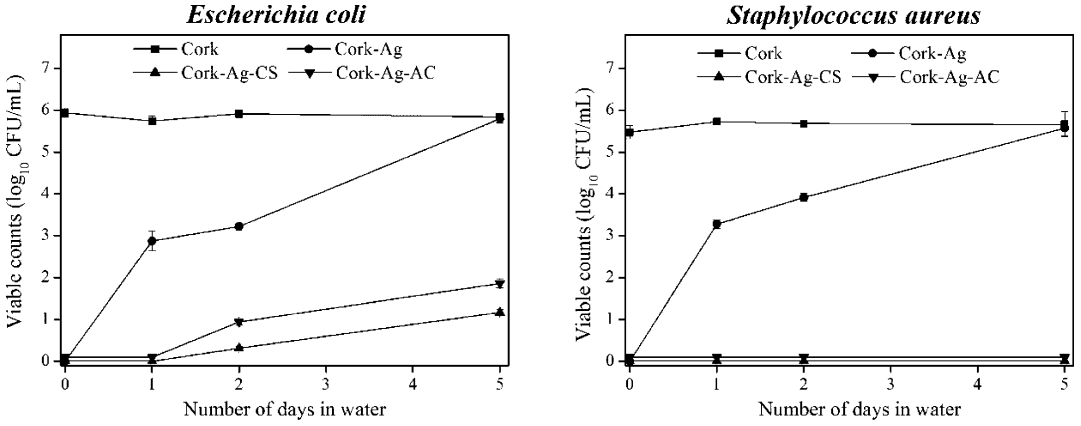

Figure 5. Antimicrobial activity of untreated and enzymatically functionalized cork with AgNP, AgNP−CS, and AgNP−AC dispersions. The materials were subjected to the washing treatment in water (stirring 100 rpm) for up to 5 days, during which the antibacterial activity is evaluated at different time points.

The results of the time-kill experiments showed that the cork matrices treated with pure AgNP (immediately upon their preparation) fully inhibited the bacterial growth for both *E. coli* and *S. aureus* if no washing procedure was performed (Figure 5). Although not expected in such an extent, the antibacterial effect of the cork−AgNP sample could be explained by a moderate adsorption capacity of cork toward silver.[34] In contrast, other materials such as nanoclay have been associated with AgNP in the absence of auxiliary molecules to impart diffusion-controlled antimicrobial activity, with long-term impact.[35] Adsorption of metals onto different sorbents may occur by physiosorption and chemisorption.[17,36] Considering that the chemisorption involves the permanent modification through generation of new chemical bonds at the surface of a material and the progressive loss of the antibacterial effect of cork—AgNP during 5 days in water occurred, it is logical to conclude that this material maintained the activity only until the physically adsorbed particles persisted on its surface. On the other hand, the cork matrices functionalized with AgNP−CS and AgNP−AC hybrids preserved most of the antibacterial effect (against *E. coli*) or fully retained the effect (against *S. aureus*) during the extensive washing procedure. Although it is probable that some of the hybrid structures were also physically adsorbed on the surface (reflected in somewhat lower effect of the cork−AgNP−CS and AgNP−AC in the case of *E. coli* after 5 days of washing), these results indirectly confirm the FTIR and SEM findings for the permanent functionalization of cork with AgNP−biopolymer hybrids using the laccase-assisted approach.

The antimicrobial effect of cork−AgNP−CS and cork−AgNP−AC after 5-day washing was also compared to the matrices enzymatically functionalized with only CS and AC (without AgNP), in order to reveal if the effect of the biopolymers was restricted only to the material functionalization. Calculated in percentage of bacterial inhibition compared to the effect of untreated cork, the matrices with enzymatically embedded hybrid AgNP−CS and AgNP−AC reduced, respectively, by 99.6% and 85.3% the growth of *E. coli*, but showing the full kill potential in the case of *S. aureus* (Table 2). Although the SEM images showed more AgNP particles immobilized on cork in the case of AgNP−CS, the antimicrobial efficiency of these two materials was comparable for the used bacteria inoculums. Such a scenario did not allow us to clearly distinguish the individual effects of AgNP on one side and intrinsically antimicrobial CS or AC on another. Indeed, CS is a known, while AC (a more economical substitute of CS) is an emerging antimicrobial macromolecule in different forms.[37,38] Cork treated with CS and AC in the absence of AgNP did not show activity against *E. coli*, whereas the efficiency for *S. aureus* reduction was of 10.2% and 4.3%, respectively. The antibacterial potential of these matrices is measured in the assay optimized to distinguish the effect of the cork embedded with AgNP (small amount of the material and high bacteria count), which certainly possess higher antibacterial activity than the biopolymers. Thus, the absence or the low extent of the antibacterial potential of the matrices treated only with biopolymers is explained with the assay conditions applied. Moreover, a slightly higher antibacterial potential of the CS-treated compared to the matrices containing AC is attributed to better grafting of the CS macromolecule compared to AC (concluded from the SEM images). Overall, the antibacterial efficiency of the cork grafted with hybrid AgNP−biopolymers is largely dependent on the presence of silver. Nevertheless, some synergistic antibacterial effect of the AgNP and the intrinsically antibacterial amino-functional biopolymers could still be envisaged, though the enhancement of antimicrobial activity in hybrid nanoscale architectures based on silver for long-term effects is not a new concept.[39]

Table 2. Antibacterial Activity of Enzymatically Modified Cork Against *Escherichia coli* and *Staphylococcus aureus* after 5 Days Washing in Water[a]

sample	*E. coli* reduction (%)	*S. aureus* reduction (%)
cork−AgNP−CS	99.6	100
cork−AgNP−AC	85.3	100
cork−CS	0	10.2
cork−AC	0	4.3

[a]The results are expressed in % of bacteria reduction compared to the untreated cork.

4. CONCLUSIONS

In this study, the laccase oxidation of the phenol moieties in cork into reactive quinones and their further reaction with nucleophilic amino groups in CS- or AC-doped AgNP was exploited to impart durable antibacterial activity onto cork matrices. The role of CS and AC biopolymers in the hybrid NP structures was 3-fold in order to (i) stabilize the AgNP and

DOI: 10.1021/acsami.5b01670
ACS Appl. Mater. Interfaces 2015, 7, 9792−9799

prevent their aggregation, (ii) serve as an interface for permanent grafting of AgNP on cork, and (iii) synergistically improve the AgNP antibacterial effect. The biocatalytically functionalized cork matrices with AgNP−CS and AgNP−AC efficiently reduced the *Escherichia coli* and *Staphylococcus aureus* growth during the course of 5 days. Such long-term stability and durability of the antimicrobial effect in conditions of continuous water flow suggest the potential application of the functionalized cork matrices in constructed wetlands as an adsorbent for removal of wastewater impurities, at the same time avoiding microbial contaminations.

AUTHOR INFORMATION

Corresponding Author

*Tel.: +34937398570. Fax: +34937398225. E-mail: tzanko.tzanov@upc.edu.

Author Contributions

#These authors contributed equally to the work

Notes

The authors declare no competing financial interest.

REFERENCES

(1) Agudelo, R. M.; Peñuela, G.; Aguirre, N. J.; Morató, J.; Jaramillo, M. L. Simultaneous Removal of Chlorpyrifos and Dissolved Organic Carbon using Horizontal Sub-Surface Flow Pilot Wetlands. *Ecol. Eng.* **2010**, *36*, 1401−1408.

(2) Garcí, J.; Rousseau, D. P.; Morató, J.; Lesage, E.; Matamoros, V.; Bayona, J. M. Contaminant Removal Processes in Subsurface-Flow Constructed Wetlands: a Review. *Crit. Rev. Environ. Sci. Technol.* **2010**, *40*, 561−661.

(3) Li, Y.; Zhu, G.; Ng, W. J.; Tan, S. K. A Review on Removing Pharmaceutical Contaminants from Wastewater by Constructed Wetlands: Design, Performance and Mechanism. *Sci. Total Environ.* **2014**, *468−469*, 908−932.

(4) Casas-Zapata, J. C.; Ríos, K.; Florville-Alejandre, T. R.; Morató, J.; Peñuela, G. Influence of Chlorothalonil on the Removal of Organic Matter in Horizontal Subsurface Flow Constructed Wetlands. *J. Environ. Sci. Health, Part B* **2013**, *48*, 122−132.

(5) Phu, D. V.; Quoc, L. A.; Duy, N. N.; Hien, N. Q. Study of Incorporation of Silver Nanoparticles onto PE-g-PAAc Nonwoven Fabric by γ-Irradiation for Water Treatment. *Radiat. Phys. Chem.* **2013**, *88*, 90−94.

(6) Hossaina, F.; Perales-Perez, O. J.; Hwang, S.; Román, F. Antimicrobial Nanomaterials as Water Disinfectant: Applications, Limitations and Future Perspectives. *Sci. Total Environ.* **2014**, *466−467*, 1047−1059.

(7) Rai, M.; Yadav, A.; Gade, A. Silver Nanoparticles as a New Generation of Antimicrobials. *Biotechnol. Adv.* **2009**, *27*, 76−83.

(8) Sharma, V. K.; Yngard, R. A.; Lin, Y. Silver Nanoparticles: Green Synthesis and their Antimicrobial Activities. *Adv. Colloid Interface Sci.* **2009**, *145*, 83−96.

(9) Wang, W.; Gu, B. Preparation and Characterization of Silver Nanoparticles at High Concentrations. *ACS Symp. Ser.* **2009**, *878*, 1−14.

(10) Abdullin, T. I.; Bondar, O. V.; Shtyrlin, Y. G.; Kahraman, M.; Culha, M. Pluronic Block Copolymer-Mediated Interactions of Organic Compounds with Noble Metal Nanoparticles for SERS Analysis. *Langmuir* **2010**, *26*, 5153−5159.

(11) Bae, E.; Park, H.-J.; Park, J.; Yoon, J.; Kim, Y.; Choi, K.; Yi, J. Effect of Chemical Stabilizers in Silver Nanoparticle Suspensions on Nanotoxicity. *Bull. Korean Chem. Soc.* **2011**, *32*, 613−619.

(12) Reicha, F. M.; Sarhan, A.; Abdel-Hamid, M. I.; El-Sherbiny, I. M. Preparation of Silver Nanoparticles in the Presence of Chitosan by Electrochemical Method. *Carbohydr. Polym.* **2012**, *89*, 236−244.

(13) Ali, S. W.; Rajendran, S.; Joshi, M. Synthesis and Characterization of Chitosan and Silver Loaded Chitosan Nanoparticles for Bioactive Polyester. *Carbohydr. Polym.* **2011**, *83*, 438−446.

(14) Guo, Y.-B.; Wang, D.-G.; Liu, S.-H.; Zhang, S.-W. Fabrication and Tribological Properties of Polyelectrolyte Multilayers Containing in Situ Gold and Silver Nanoparticles. *Colloids Surf., A* **2013**, *417*, 1−9.

(15) Juan, L.; Zhimin, Z.; Anchun, M.; Lei, L.; Jingchao, Z. Deposition of Silver Nanoparticles on Titanium Surface for Antibacterial Effect. *Int. J. Nanomed.* **2010**, *5*, 261−267.

(16) Jové, P.; Olivella, M. À.; Cano, L. Study of the Variability in Chemical Composition of Bark Layers of Quercus Suber L. from Different Production Areas. *BioResources* **2011**, *6*, 1806−1814.

(17) Pintor, A. M.; Ferreira, C. I.; Pereira, J. C.; Correia, P.; Silva, S. P.; Vilar, V. J.; Botelho, C. M.; Boaventura, R. A. Use of Cork Powder and Granules for the Adsorption of Pollutants: a Review. *Water Res.* **2012**, *46*, 3152−3166.

(18) Chubar, N.; Carvalho, J. R.; Correia, M. J. N. Cork Biomass as Biosorbent for Cu(II), Zn(II) and Ni(II). *Colloids Surf., A* **2003**, *230*, 57−65.

(19) Olivella, M. À.; Jové, P.; Bianchi, A.; Bazzicalupi, C.; Cano, L. An Integrated Approach to Understanding the Sorption Mechanism of Phenanthrene by Cork. *Chemosphere* **2013**, *90*, 1939−1944.

(20) Teixeira, L. S. M.; Feijen, J.; Blitterswijk, C. A. v.; Dijkstra, P. J.; Karperien, M. Enzyme-Catalyzed Crosslinkable Hydrogels: Emerging Strategies for Tissue Engineering. *Biomaterials* **2012**, *33*, 1281−1290.

(21) Aracri, E.; Blanco, C. D.; Tzanov, T. An Enzymatic Approach to Develop a Lignin-Based Adhesive for Wool Floor Coverings. *Green Chem.* **2014**, *16*, 2597−2603.

(22) Hossai, K. M. G.; González, M. D.; Juan, A. R.; Tzanov, T. Enzyme-Mediated Coupling of a Bi-Functional Phenolic Compound onto Wool to Enhance its Physical, Mechanical and Functional Properties. *Enzyme Microb. Technol.* **2010**, *46*, 326−330.

(23) Blanco, C. D.; González, M. D.; Monmany, J. M. D.; Tzanov, T. Dyeing Properties, Synthesis, Isolation and Characterization of an in Situ Generated Phenolic Pigment, Covalently Bound to Cotton. *Enzyme Microb. Technol.* **2009**, *44*, 380−385.

(24) Blanco, C. D.; Ortner, A.; Dimitrov, R.; Navarro, A.; Mendoza, E.; Tzanov, T. Building an Antifouling Zwitterionic Coating on Urinary Catheters Using an Enzymatically Triggered Bottom-Up Approach. *ACS Appl. Mater. Interfaces* **2014**, *6*, 11385−11393.

(25) Rocasalbas, G.; Francesko, A.; Touriño, S.; Fernández-Francos, X.; Guebitz, G. M.; Tzanov, T. Laccase-Assisted Formation of Bioactive Chitosan/Gelatin Hydrogel Stabilized with Plant Polyphenols. *Carbohydr. Polym.* **2013**, *92*, 989−996.

(26) Huang, H.; Yuan, Q.; Yang, X. Preparation and Characterization of Metal−Chitosan Nanocomposites. *Colloids Surf., B* **2004**, *39*, 31−37.

(27) Cheng, F.; Betts, J. W.; Kelly, S. M.; Schaller, J.; Heinze, T. Synthesis and Antibacterial Effects of Aqueous Colloidal Solutions of Silver Nanoparticles Using Aminocellulose as a Combined Reducing and Capping Reagent. *Green Chem.* **2013**, *15*, 989−998.

(28) Rahn, K.; Diamantoglou, M.; Klemm, D.; Berghmans, H.; Heinze, T. Homogeneous Synthesis of Cellulose p-Toluenesulfonates in N,N-Dimethylacetamide/LiCl Solvent System. *Angew. Makromol. Chem.* **1996**, *238*, 143−163.

(29) Petkova, P.; Francesko, A.; Fernandes, M. M.; Mendoza, E.; Perelshtein, I.; Gedanken, A.; Tzanov, T. Sonochemical Coating of Textiles with Hybrid ZnO/Chitosan Antimicrobial Nanoparticles. *ACS Appl. Mater. Interfaces* **2014**, *6*, 1164−1172.

(30) George, J.; Kumar, R.; Sajeevkumar, V. A.; Ramana, K. V.; Rajamanickam, R.; Abhishek, V.; Nadanasabapathy, S.; Siddaramaiah. Hybrid HPMC Nanocomposites containing Bacterial Cellulose Nanocrystals and Silver Nanoparticles. *Carbohydr. Polym.* **2014**, *105*, 285−292.

(31) Tran, H. V.; Tran, L. D.; Ba, C. T.; Vu, H. D.; Nguyen, T. N.; Pham, D. G.; Nguyen, P. X. Synthesis, Characterization, Antibacterial and Antiproliferative Activities of Monodisperse Chitosan-based Silver Nanoparticles. *Colloids Surf., A* **2010**, *360*, 32−40.

DOI: 10.1021/acsami.5b01670
ACS Appl. Mater. Interfaces 2015, 7, 9792−9799

(32) Lopes, M. H.; Barros, A.; Neto, C. P.; Rutledge, D. N.; Delgadillo, I.; Gil, A. M. Variability of Cork from Portuguese Quercus Suber Studied by Solid-State 13C-NMR and FTIR Spectroscopies. *Biopolymers* **2001**, *62*, 268−277.
(33) Lopes, M. H.; Neto, C. P.; Barros, A.; Rutledge, D. N.; Delgadillo, I.; Gil, A. M. Quantitation of Aliphatic Suberin in Quercus Suber L. Cork by FTIR Spectroscopy and Solid-State 13C-NMR Spectroscopy. *Biopolymers* **2000**, *57*, 344−351.
(34) Hanzlík, J.; Jehlička, J.; Šebek, O.; Weishauptová, Z.; Machovič, V. Multi-Component Adsorption of Ag(I), Cd(II) and Cu(II) by Natural Carbonaceous Materials. *Water Res.* **2004**, *38*, 2178−2184.
(35) Girase, B.; Depan, D.; Shah, J. S.; Xu, W.; Misra, R. D. K. Silver−Clay Nanohybrid Structure for Effective and Diffusion-Controlled Antimicrobial Activity. *Mater. Sci. Eng., C* **2011**, *31*, 1759−1766.
(36) Witek-Krowiak, A.; Szafran, R. G.; Modelski, S. Biosorption of Heavy Metals from Aqueous Solutions onto Peanut Shell as a Low-Cost Biosorbent. *Desalination* **2011**, *265*, 126−134.
(37) Genco, T.; Zemljič, L. F.; Bračič, M.; Stana-Kleinschek, K.; Heinze, T. Physicochemical Properties and Bioactivity of a Novel Class of Cellulosics: 6-Deoxy-6-Amino Cellulose Sulfate. *Macromol. Chem. Phys.* **2012**, *213*, 539−548.
(38) Fernandes, M. M.; Francesko, A.; Torrent-Burgués, J.; Carrión-Fité, F. J.; Heinze, T.; Tzanov, T. Sonochemically Processed Cationic Nanocapsules: Efficient Antimicrobials with Membrane Disturbing Capacity. *Biomacromolecules* **2014**, *15*, 1365−1374.
(39) Misra, R. D. K.; Girase, B.; Depan, D.; Shah, J. S. Hybrid Nanoscale Architecture for Enhancement of Antimicrobial Activity: Immobilization of Silver Nanoparticles on Thiol-Functionalized Polymer Crystallized on Carbon Nanotubes. *Adv. Eng. Mater.* **2012**, *14*, B93−B100.

DOI: 10.1021/acsami.5b01670
ACS Appl. Mater. Interfaces 2015, 7, 9792−9799